International Journal of Nanoelectronics and Materials
Volume 15, No. 1, January 2022 [37-52]

Fabrication of Cobalt Ferrite Nanoparticles with a Facile Approach: Variations in Structural, Dielectric and Morphological Properties by Influence of Annealing Temperature

Naimatullah Channa[1], Nasir Abbas[2], Junaid Kareem Khan[3], Muhammad Khalid[4*], Malik Muhammad HafeezUllah[5], Muhammad Kashif[4], Sehrish Inam[4], Maria Arshad[4]

[1]Department of Physics, Shah Abdul Latif University Khairpur 66111, Pakistan
[2]Department of Applied Physics, University of Karachi, 75270, Karachi, Pakistan
[3]Department of Physics, NED University of Engineering and Technology, 75270, Karachi, Pakistan
[4]Department of Physics, University of Karachi, 75270, Karachi, Pakistan
[5]Department of Mathematics, Balochistan University of Information Technology, Engineering and Management Sciences, Quetta, Pakistan

Received 9 September 2021, Revised 30 September 2021, Accepted 19 October 2021

ABSTRACT

Spinel ferrites have a significant impact due to its physical and chemical properties. The sol-gel route has been employed in the present work, for achieving single phase nano-crystalline cobalt ferrites. All these samples were annealed with different temperatures from 600 °C to 900 °C in a muffle furnace. The FCC spinel structure of nanoparticles has been confirmed by powder x-ray diffraction (XRD) studies that demonstrate formation of crystalline size at various temperatures from 11–15 nm. The Raman spectroscopy revealed the characteristic absorption bands in 100 cm^{-1} to 700 cm^{-1} range where the graphs show five absorption bands and they confirmed the characteristic feature of spinel structure. With the help of Maxwell Wagner model, dielectric characterization has been carried out within a frequency range from 20 Hz to 20 MHz where dielectric parameters are found decreased with increasing the applied frequency. The alternating current conductivity phenomena increases with higher frequency ranges and show plane behavior in lower frequency ranges. The impedance mechanism, real and imaginary parts show decreasing trend on account of grain boundary activity. Interfacial polarization understood with the help of peaks obtained from the imaginary modulus pattern. These cobalt ferrite nanoparticles ($CoFe_2O_4$ NPs*) are suitable to use in microwave devices, high frequency equipment, semiconductor devices and high storage media applications revealed by the dielectric studies.*

Keywords: Nanoparticles, Raman spectroscopy, Spinel ferrites, Sol-gel

1. INTRODUCTION

The ferrites have polycrystalline structure and exhibit excellent physical properties due to high permeability, high resistivity, low power losses and suitable chemical stability [1, 2]. Therefore, these materials have potential applications in industries for fabrication of transformer cores, drug delivery devices, cancer treatment equipment, microwave devices, magnetic resonance imaging (MRI) and E. M. wave absorbers [3-7]. These significant characteristics of spinel's are obtained by their chemical

*Corresponding author: mkhalid@uok.edu.pk

composition, annealing temperature, fabrication route, nature of dopant and site occupancy of dopant [8]. During the last decades, researchers are showing potential interest in exhibiting the materials to enhance the physical properties at nano level which is completely different when compared with bulk materials. These composites such as barium titanate/cobalt ferrite, the combination of spinel ferrites with ceramic materials attract the most researchers and scientists for multifunctional applications in present days [9, 10]. Nowadays, advanced research in the field of ceramic materials has changed the digital world and plays a vital role for new inventions in each year which have brought about a revolution [11]. However, in order to understand the concept about the properties of these nanoscale materials like capacitance of a dielectric material, the first important point is to know about the nature of dielectric [12]. Under the applied electric field, materials exhibit polarization behavior due to the dipoles aligned in applied field direction, where it has been revealed that the applied frequency is a major factor for significant changes in the material dielectric constant [13]. The study of dielectric loss because of DC resistivity is playing a vital role for ceramic materials, the ionic transition between the lower energy states to the higher energy states take place mainly at high frequency ranges or dielectric loss phenomena may be on account of the dipole rotation [14]. In molecular dielectric, the maximum value of polarization is dependent on the time taken for alignments of adjacent molecules along with external applied frequency. This mechanism is termed as dielectric relaxation, which is an essential characteristic of relaxer ceramic materials [15]. Nowadays, the significant insulating properties of dielectric materials put them for consideration of various applications in different fields and these properties are actually depending on the insulating parameters such as high electrical resistivity and low dielectric loss.

Ferrites are oxides materials possessed with two crystallographic sites, tetrahedral site and octahedral site denoted by "A" and "B" respectively [16]. The cobalt ferrite exhibits spinel structure, where Fe^{3+} ions are evenly spaced at both A and B sites and Co^{2+} ions engage A sites of lattice. Nevertheless, the behavior of nano sized cobalt ferrites depends upon occupancy and number of Co^{2+} and Fe^{3+} ions present at lattice sites and fabrication route [17-20]. Recently, researchers are interested in developing nano sized ferrite through a simple, cost effective and environment friendly route known as sol-gel self-combustion route [21]. Cobalt ferrite nanoparticles have been prepared by Honey mediated, the structural variations and grain size influence on different physical properties like magnetic, electric, relaxation, dielectric and impedance [9]. It has been investigated that the particle size is depending upon sintered temperature [22]. Further, the drastic changes in the dielectric and magnetic properties in ferrites are influenced by fabrication technique and particle size [23, 24]. The saturation magnetization, retentivity and coercivity were affected by particle size whereas dielectric properties are decreased by annealing temperature. Furthermore, the cobalt ferrites exhibit supercapacitor capability at low scan rate [25]. The dielectric properties are decreased whereas AC conductivity is increased with frequency. Velhal et al. prepared the nickel-cobalt nanoferrite and they observed a dispersion trend of the dielectric constant with effect of applied field. They also determined high resistance due to the semi-circle nature of the impedance spectrum [26].

In the present work, sol-gel auto combustion method has been employed for synthesis of cobalt ferrite nanoparticles. The structural and morphological properties are observed by a diffractometer (XRD). Electrical, dielectric and other properties were investigated by different characterization techniques such as Scanning Electron Microscope (SEM), Impedance Analyzer and Raman spectroscopy. Furthermore, the effects of grains and grain boundaries on the electric and dielectric properties were carried out through modulus and impedance spectroscopy.

2. EXPERIMENTAL PROCEDURE

Cobalt ferrite nanoparticles which are temperature dependent were fabricated by using sol-gel auto combustion process [27]. In the present work, the mixture is consists of citric acid, iron nitrate and cobalt nitrate compounds [28]. The mixture was then introduced in distilled water to prepare solution by considering a stoichiometric ratio of cobalt nitrate, iron nitrate and citric acid. After that, the beaker was placed on the hotplate to provide continuous stirring for 30 minutes in order to obtain a homogeneous and clear solution. Later, citric acid was mixed in aqueous solution and heated at 150 ^{0}C with stirring for 2 hours on a hot plate and as a product, dry powder was obtained. The powder was grinded smoothly and finally converted into homogenous and fluffy powder. By using a hydraulic press, this nano-powder was pelletized and further annealed at different temperatures (600 ^{0}C to 900 ^{0}C) about three hours for purification and form the required cobalt ferrite nanoparticles.

3. CHARACTERIZATION TECHNIQUES

Various characterizations, for noticing structural parameters, morphological, electrical and other characteristics, were done with different investigation tools. The X-Ray Diffractometer, manufactured by PANalytical X'Pert Pro software has been used to identify the phase orientation of prepared ferrite samples with incident Cu-Kα source radiation having λ of 0.154156 nm. The morphological study was noticed with the assistance of FEI NOVA 450 NanoSEM. The electrical characteristics of ferrites were noticed with the assistance of 6520P Wayne Kerr LCR meter. For this purpose, temperature dependent ferrites were pelletized having diameter 3.75 mm and thicknesses of 3.5 mm. Frequency dependent dielectric measurements were carried out, the data has been measured at a wide frequency span from 20 Hz-20 MHz. The current of 5 mA is applied to the prepared pellets.

4. RESULTS AND DISCUSSION

4.1 Structural Analysis

The structural analysis of the present samples has been confirmed by XRD technique. The source radiations are incident on samples; the retained data was calculated, depicted XRD curves and finally indexed. The presence of hkl planes were observed such that (111), (220), (311), (222), (400), (422), (511), (440), (622) as depicted in Figure 1. The indexing of XRD graph figures verified that the structure of prepared nanoparticles is spinel structure and all observed peaks at corresponding angle matched with standard JCPDS# 22-1086 [29]. All mentioned diffraction patterns confirm that prepared samples have cubic spinel structure. With the help of Scherrer formula, the size of crystallite has been calculated, however, it has been observed maximum 26.09 nm, at annealing temperature 900 °C and minimum 23.79 nm at 600 °C. Increasing in size of nanoparticles leads to a low signal to noise ratio due to decreasing magnetic properties of such materials.

$$d_{hkl} = \frac{0.89\lambda}{B\cos\theta} \tag{1}$$

Here, d is particle size, 0.89 is the value of constant K known as shape factor, λ is the wavelength of X-rays and θ is diffraction angle. The lattice constant (a) was determined by the following equation:

$$a = d_{hkl}\sqrt{h^2 + k^2 + l^2} \tag{2}$$

where (hkl) represents the Miller indices. The other parameters dislocation (δ) density and stacking fault (SF) is determined by:

$$\delta = \frac{1}{D^2} \tag{3}$$

$$SF = \frac{2\pi^2}{45\sqrt{3tan\theta}} \tag{4}$$

and the lattice strain and microstrain were determined as in the following relations:

$$\varepsilon_{lattice} = \frac{\beta}{4\tan\theta} \tag{5}$$

$$\varepsilon_{micro} = \frac{\beta\cos\theta}{4} \tag{6}$$

In the above equations, $\varepsilon_{lattice}$ and ε_{micro} is the lattice strain and microstrain respectively, β is full width half maxima and θ is diffraction angle. The summary of the above parameters [30, 31] is shown in Table 1.

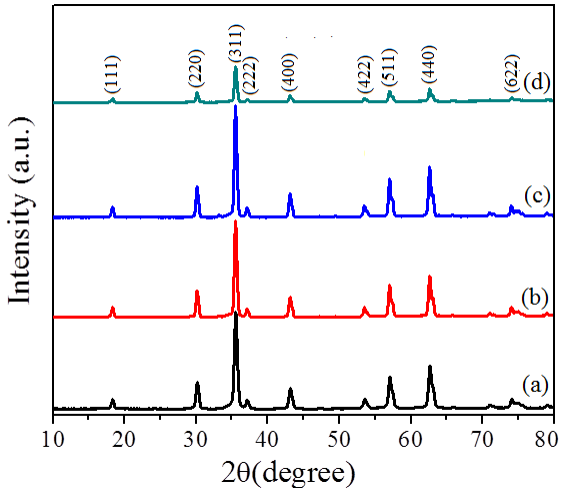

Figure 1. The XRD patterns at various temperatures (a) 600 °C (b) 700 °C (c) 800 °C and (d) 900 °C of prepared cobalt ferrite nanoparticles

The crystallite size and microstrain of the prepared cobalt samples were understood through Williamson Hall Method [32]. The diffracted beams were observed sharper by increasing annealing temperature that confirms the stable crystal structure. The calculated data depicts that the lattice constant slightly increased by increasing annealed temperature whereas size of crystallite have inverse effect excluding at 900 °C where the crystallite size has found maximum 26.09603 nm. The increasing effect in lattice constant is as account on increased in annealing temperature, which follows the Vegdar's Law [33]. This effect is appeared to reordering of cations arrangement in the ferrites and under the applied annealing temperatures all other parameters, as mentioned in the Table 1, confirmed that the prepared material has stable cubic spinel structure. All these structural parameters have changed nearly the same order with increasing in annealing temperature from 600 - 800 °C and varied at 900 °C.

Table 1. Temperature dependent structural parameters of cobalt ferrite nanoparticles

Annealing temperature	Lattice constant	Crystallite size	Dislocation density	Lattice strain	Micro strain x 10^{-3}	Stacking fault

(^{0}C)	a = b = c (Å)	(nm)	x 10^{-15} (lines/m^2)	x 10^{-3}	(lines^{-2}/m^{-4})	
600	8.36448	25.86463	0.001495	4.632	1.414	0.44737
700	8.370652	24.7024	0.001639	4.853	1.481	0.44755
800	8.371948	23.7952	0.001766	5.039	1.537	0.44759
900	8.372141	26.09503	0.001469	4.595	1.402	0.44760

4.2 Morphological Studies

Scanning electron microscope (SEM) has been employed to investigate the surface morphology of cobalt ferrite nanoparticles fabricated through sol-gel self-combustion route at different annealing temperatures (600 °C to 900 °C). Figure 2 shows that temperature dependent grain size and their distribution. Furthermore, It is clear that grain are agglomerated and tightly connect with each other due to its magnetic nature of cobalt ferrite nanoparticles.

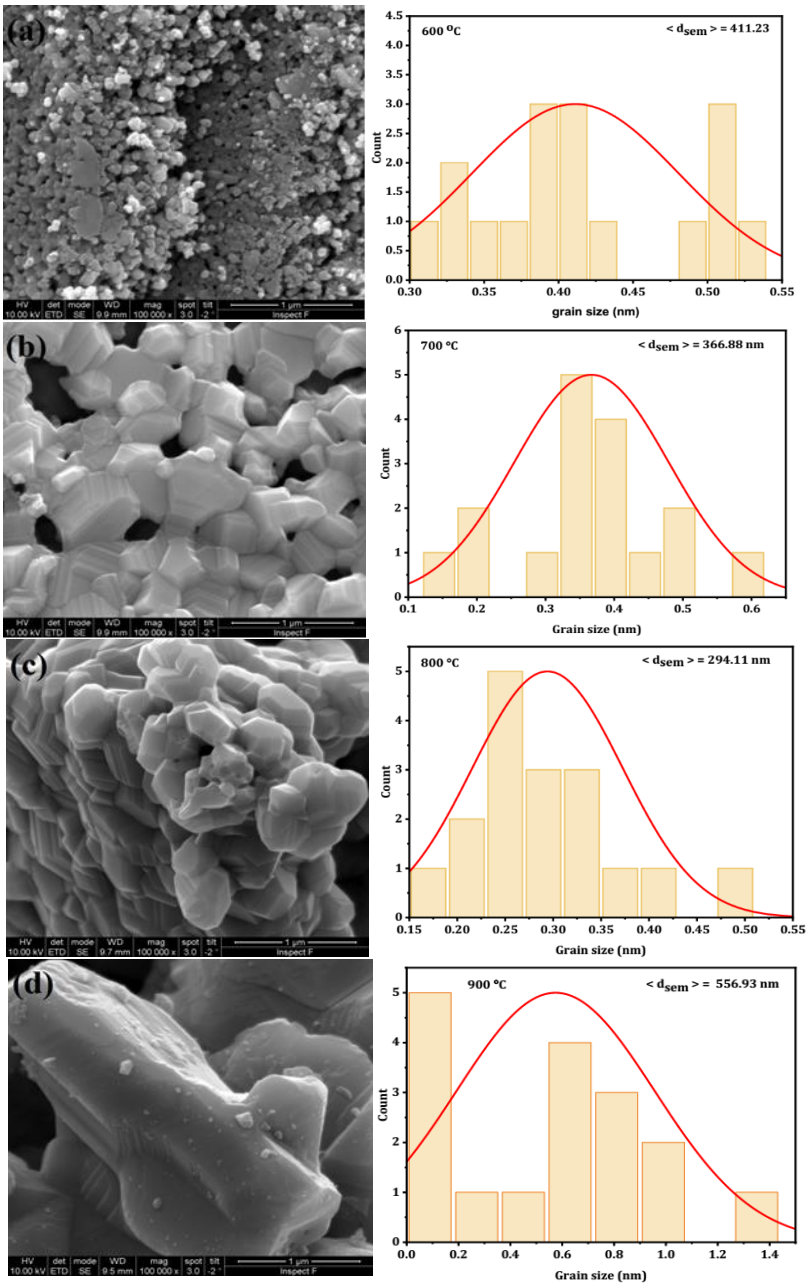

Figure 2. Images (a-d) obtained from SEM micrographs of the cobalt ferrite nanoparticles

The different rectangular shapes and irregular morphology observed in these microstructures. This behavior may occur due to diffusivity methods. Cobalt ferrites depict spherical agglomerate structure at annealing temperature of 600 °C, due to exaggerated particle growth. Generally, ferrites show such spherical agglomerate phenomenon and has already been reported in different authors. As the grains are composed of several particles, , this divergence appears in the images, due to internal stress or the defects produced in nanostructure.

4.3 Dielectric Analysis

Temperature dependent dielectric parameters of cobalt ferrite nanoparticles were observed through the 6520P Wayne Kerr LCR meter. The thickness of pellets was 1.25 mm and having diameter of 7.5 mm. Frequency dependent dielectric measurements were carried out, between applied frequency ranges from 20 Hz to 20 MHz with current 5 mA. Following specifications has been determined from the analysis of obtained data.

4.3.1 Dielectric (Real and Imaginary) Constants

In the dielectric constants, the appearance of a high dispersion phenomena at low frequency ranges are due to the electronic exchange between metallic ions with different oxidation states, i.e., Fe^{3+} and Fe^{2+}. It is explained in Koop's theory [34], that preimages to nano samples have an inhomogeneous structure of two layers of Maxwell Wagner Model [35]. In Figure 3, it is clearly seen that the real part of dielectric constant of all samples show high dispersion at lower frequency ranges, decrease gradually and finally saturated at high frequency range. As increasing in annealing temperature, the real part of dielectric constant is also increased till 800 °C due to contribution of grain boundaries but at 900°C, value of dielectric constant is minimized owing to grain contribution, i.e., conduction mechanism. The grain boundaries offer resistance whereas grain offers conduction.

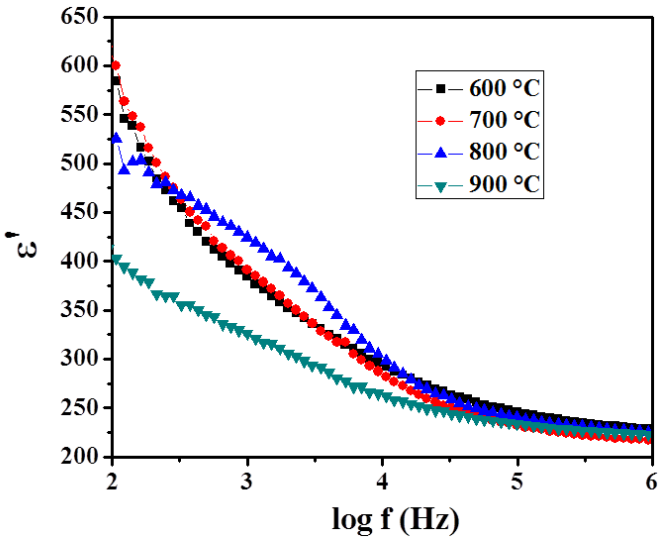

Figure 3. Real part of dielectric constant versus frequency for cobalt ferrite nanoparticles, annealed at various temperatures from 600 °C to 900°C

The presence of polarization behavior in spinel is analogous to the conduction mechanism associated with electron hopping phenomenon in the cobalt ferrites. Thus, grain boundaries play a vital role to provide resistance and thereby, polarization behavior is dominant at lower frequency ranges. But at higher frequencies, reduction trend is observed in polarization behavior by reason of the electron which is not associated with applied electric field frequency. Figure 4 displays that the complex dielectric constant has larger magnitude at lower annealing temperature values and reduction at higher temperature. At 900 °C, irregular changes are observed which associated with inhomogeneous morphological features of nanoparticles.

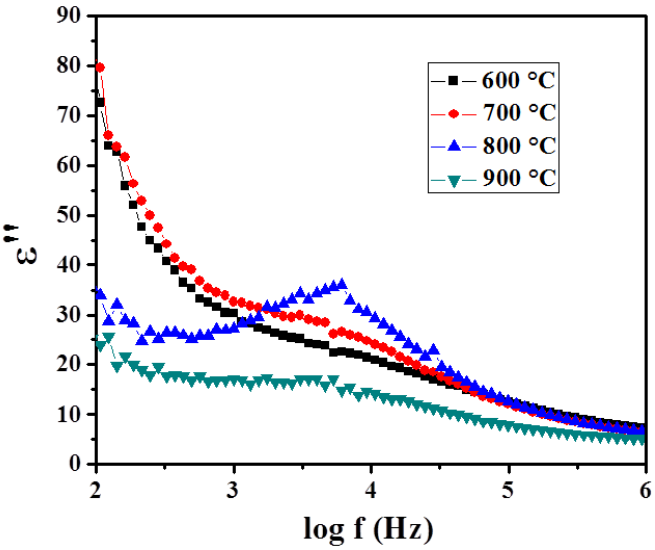

Figure 4. Complex dielectric constant patterns of cobalt ferrite nanoparticles at various temperatures from 600 °C to 900 °C with frequency dependency

The frequency dependent dielectric constants ε′ and ε′′ at frequencies of 10 kHz, 50 kHz and 20 MHz are depicted in Table 2. It has been noticed that the value of real part is varied from 262 to 298 at 10 kHz; 239 to 356 at 50 kHz and 252 to 609 at 20 MHz whereas the value of imaginary is varied from 14 to 29 at 10 kHz; 9 to 16 at 50 kHz and 49 to 58 at 20 MHz. These parameters are varied due to cations distribution at tetrahedral and octahedral sites, microstructure variations and grain size of crystallite [15].

4.3.2 Dielectric Tangent Loss (tanδ)

The dielectric loss in polycrystalline ferrites is due to contribution of grain boundaries, impurities and imperfections in the spinel structure. In nano structures, these inhomogeneities induce an absorption current on account of space charge which is correlated with dielectric loss. Another reason may be due to the presence of gaseous absorption like oxygen and hydrogen by surface layer bonds which are highly reactive and cause an increase in dielectric loss. The maximum peak observed in the tangent loss indicates that the hopping frequency of charge carriers and applied frequency are resonated [30]. In the spinel, conduction process occurs due to n type as well as p type charge carriers. The occurrence of n type charge flow is due to electronic hopping between divalent and trivalent Fe ions whereas occurrence of p type charge flow because of the hopping of charges amid Co^{2+} and Co^{3+} ions. The Debye relaxation mechanism appears when the hopping charge carrier's frequency is resonated to the applied frequency.

The values of dielectric loss are tabulated in Table 2 in the span of 10 KHz, 50 kHz and 20 MHz. In this work, variations in estimated value of tangent loss are 0.054 to 0.098 at 10 kHz, 0.040 to 0.066 at 50 kHz and 0.085 to 0.095 at 20 MHz. Therefore, prepared cobalt ferrites are extensively used in microwave application due to low tangent losses.

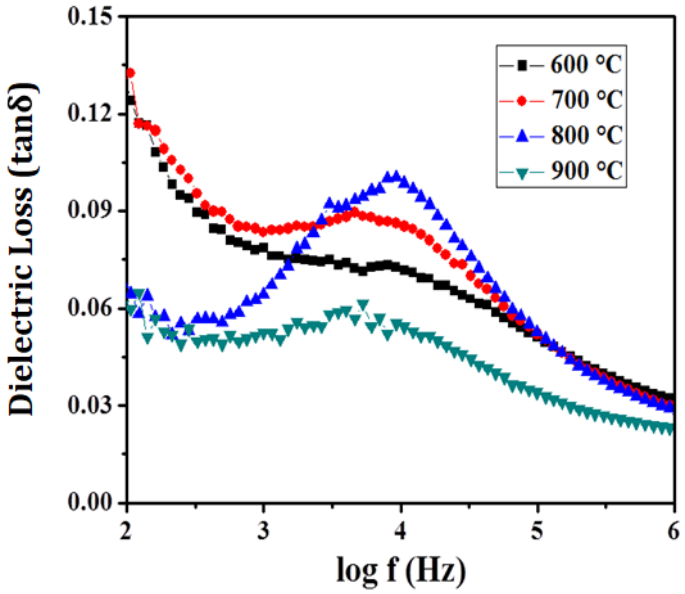

Figure 5. Patterns at different temperatures from 600 °C to 900 °C of frequency dependent dielectric loss for cobalt ferrite nanoparticles

Table 2. Different properties investigated from dielectric analysis of *cobalt ferrite* nanoparticle samples annealed at various temperature ranges from 600 °C to 900°C

Parameters	600 °C			700 °C			800 °C			900 °C		
	10kHz	50kHz	20MHz	10kHz	50kHz	20MHz	10kHz	50kHz	20MHz	10kHz	50kHz	20MHz
(Ɛ′)	291.7	255.8	552.6	281.6	241.2	552.4	298.1	249.5	609.1	262.4	239.1	588.3
(Ɛ")	20.92	14.99	48.84	24.00	15.25	47.58	29.40	16.49	58.42	14.24	9.58	50.08
Tan(δ)	0.071	0.058	0.088	0.085	0.063	0.086	0.098	0.066	0.095	0.054	0.040	0.085
(M′) (x 10^{-3})	3.41	3.89	1.795	3.52	4.12	1.797	3.32	3.99	1.62	3.80	4.17	1.68
(M") (x 10^{-3})	5.11	3.42	7.75	7.21	3.98	7.36	9.63	4.34	9.11	2.93	1.60	7.19
(Z') (kΩ)	32.6	6.56	0.0113	40.1	7.50	0.0110	43.7	7.58	0.0111	27.5	4.81	0.010
(Z″) (kΩ)	455	112	0.128	470	119	0.128	443	115	0.116	507	112	0.120

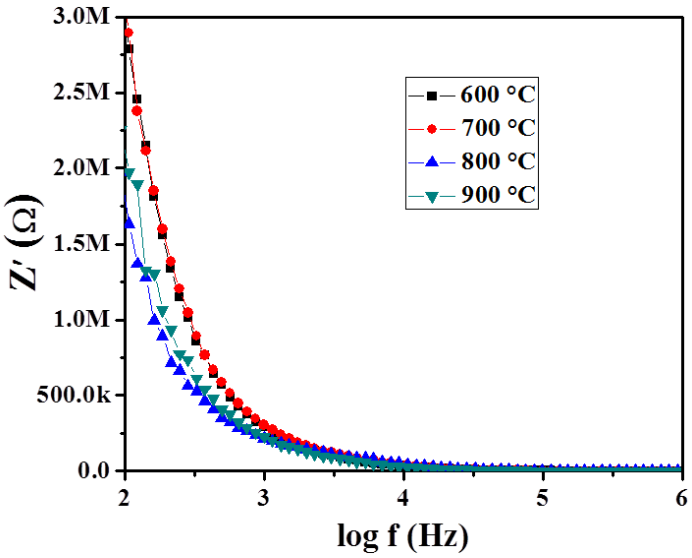

Figure 6. Patterns of real part of impedance versus applied frequency for cobalt ferrite nanoparticles

The frequency-dependent real part of impedance of prepared samples shows the variation with the increase in annealing temperature as it is enhanced at lower temperature values and can be seen in Figure 6. It means the releasing of a small number of space charges associated with annealing temperature variations. The hopping of electrons is related to the applied frequency which increases the conduction mechanism. Furthermore, Figure 6 depicts the real impedance loss (Z′) with spectrum loss that occurs with higher applied frequencies of AC electric field. This kind of trend in graphs indicates the enhancement of conduction behavior in the product. The complex impedance loss of cobalt ferrite annealed at various temperatures is plotted in Figure 7, where annealing temperature of higher value shows more complex impedance loss than lower values on applied frequency.

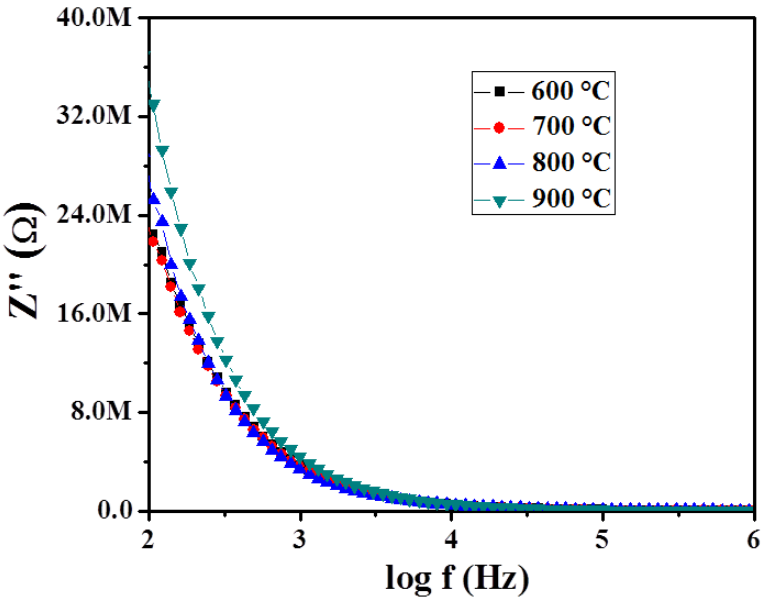

Figure 7. Patterns at various temperatures from 600 °C to 900 °C of frequency dependent complex impedance for cobalt ferrite nanoparticles

4.3.3 Electric Modulus Properties

The conductive behavior of grains and grain boundaries in ionic conductors and polycrystalline ceramics can be understood with the help of time relaxation phenomena. The variation in frequency dependent time relaxation characteristics, the contribution of conductive grains and low conductive grain boundaries variation, introducing of the hopping phenomenon amid Fe^{2+} and Fe^{3+} charges. Hence, it is significant to know conduction behavior is associated with grains or grain boundaries. For this, the frequency dependent relative modulus (M′) and complex modulus (M′′) spectroscopy plots are predominantly significant techniques to analyze relaxation phenomenon and contribution of grains and grain boundaries in transporting characteristics of charge carriers. Due to shorter mobility of charges in conduction mechanism that the patterns of real modulus (M') are disbursed at lower frequencies side and saturated at higher frequencies side as depicted in Figure 8. It is also noticed that M' shifts towards lower frequency by increasing sintering temperature. This happens because of the absence of restoring force that suggests the less influence of electrode polarization in the product [36].

The variation in the spectral peaks of complex modulus (M′′) with applied frequency of AC electric field depicts in the Figure 9, where it is noticed that asymmetric peak broadening at particular frequency reveals conductivity in the product which reinforces non-Debye type conduction mechanism [37]. It is observed in frequency dependent complex modulus (M") that the asymmetric peaks are enhanced at lower centering temperature ranges, that is due to reduction in contribution of grain size and increment in contribution of grain boundaries this phenomenon correlate with the number of dipoles in the grain boundaries in the product. Therefore, relaxation peak position shifts toward lower frequencies with increased centering temperature due to growth in interplay dipoles moment inside the grain boundaries that reduces dipole relaxation characteristics with lower relaxation frequency.

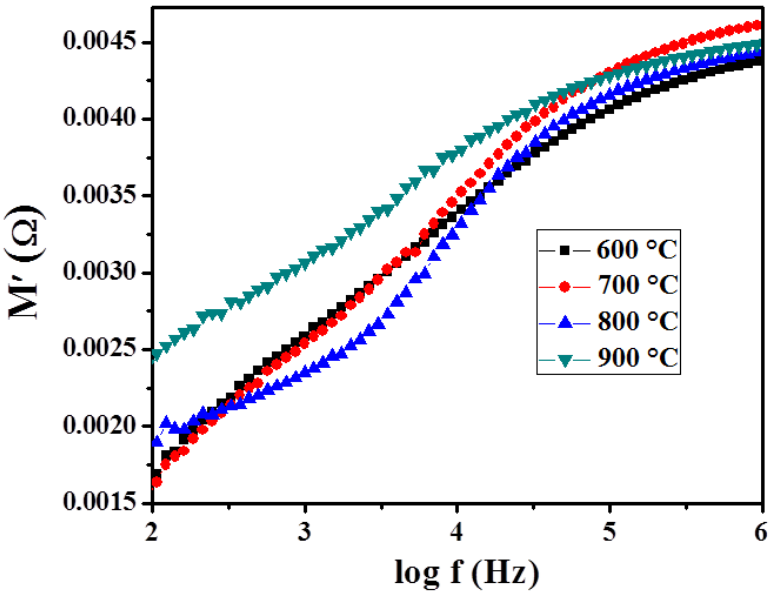

Figure 8. Patterns at various temperatures from 600 °C to 900 °C of frequency dependent real part of electric modulus for cobalt ferrite nanoparticles

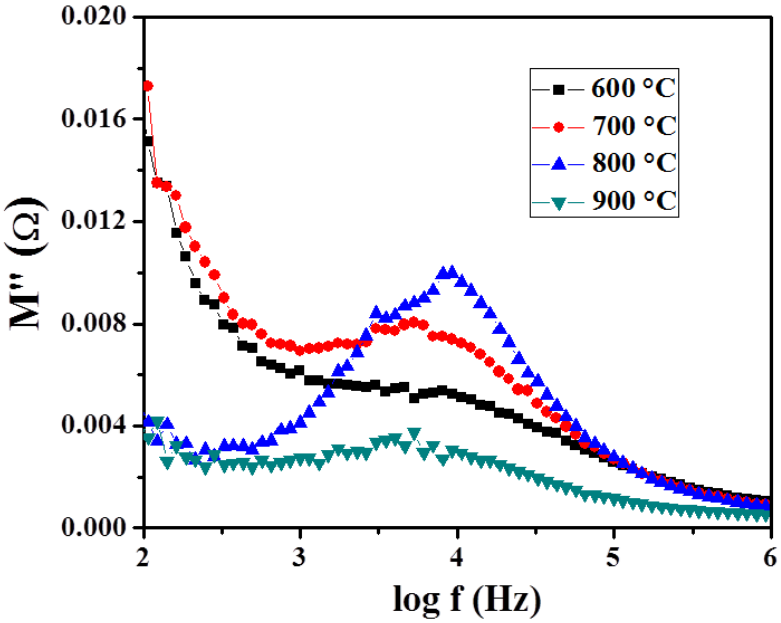

Figure 9. Patterns at various temperatures from 600 °C to 900 °C of frequency dependent imaginary part of electric modulus for cobalt ferrite nanoparticles

4.4 Raman Spectroscopy

The Raman spectroscopy is a distinguished characterization technique that provides assistance for atomic structure examination of ferrites [38]. The Raman spectra of cobalt ferrite nanoparticles are depicted in Figure 10. The less energetic photons and phonons distribution are $5T_{1u} + A_{1g} + E_g + 3T_{2g}$was noticed with assistance of Group theory analysis, where, $5T_{1u}$ modes pretend to infra-red active modes while all other $A_{1g} + E_g + 3T_{2g}$ modes pretend to be Raman active modes that depict due to Oxygen ions of lattice sites ions in the ferrites [39]. In addition, A_{1g} mode depicts because of symmetric Oxygen anion (O^+) stretching, E_g mode is achieved due to symmetric O^+ reduction whereas T_{2g} mode is produced because of asymmetric expansion of O^+ ion lieu of A sites and B sites [35]. Figure 10 is evident that Raman active modes, in cobalt ferrites, are imposed at ~198, ~297, ~461, ~558, ~604 and ~680 cm^{-1}. The Raman active mode at ~680 cm^{-1} looks like a shoulder at minimum wavenumber side. These active modes are present due to stretching vibration of $F - O$ and $M - O$ at tetrahedral sites that replicates $A_{1g}(1)$ and $A_{1g}(2)$ modes while stretching vibration of spinel structure replicates T_{2g} and E_g modes; appeared at ~198, ~297 and~461 cm^{-1}. In Figure 10, it is also noticed that Raman shift is observed by increasing annealing temperature. This phenomenon appears due to increasing size of particles and cation's redistribution in cobalt ferrites [40]. It is observed by comparison of relative intensities of $A_{1g}(1)$ with $A_{1g}(2)$ modes. Similar effect is also found with higher annealing temperature values.

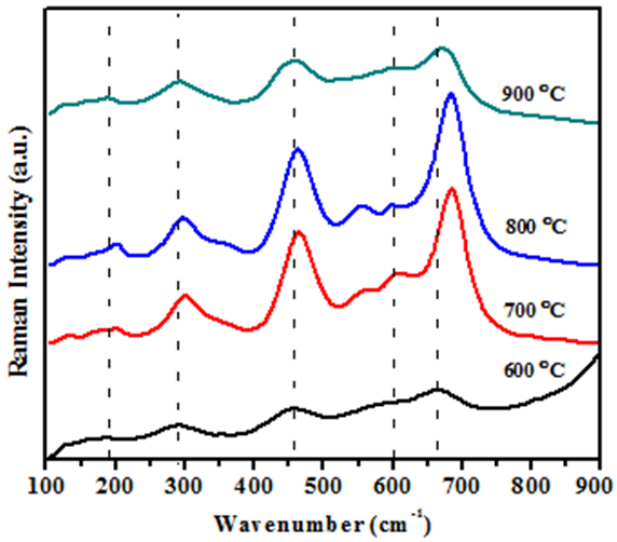

Figure 10. Raman spectroscopy of cobalt ferrite nanoparticles at various temperatures from 600 ^{0}C to 900 ^{0}C

5. CONCLUSION

Pure phase of cobalt ferrite nanoparticles with annealing temperature 600 ^{0}C, 700 ^{0}C, 800 ^{0}C and 900 ^{0}C have been achieved through sol gel self-combustion route. The impact of varied annealing temperature on the structural, morphological and electrical properties of cobalt ferrites were investigated through XRD, SEM and dielectric measurements. It is noticed through XRD that particle size is reduced with increasing annealing temperature and particle size ranges 23 nm to 26 nm has been found. The lattices constant has matched with standard value of cobalt ferrites. SEM images revealed irregular morphological properties due to thermal activation of cations super-exchange. LCR meter helps to study dielectric as well as electric parameters; it was observed that dielectric constant is decreased at high annealing temperature due to conduction of grains. The study of temperature and frequency dependent parameters of samples such as dielectric constant, tangent loss, impedance analysis and modulus, were observed and convinced that all these parameters were dips in by increasing frequency and shoots up by increasing annealing temperature. Therefore, prepared ceramic powder is suitable to be used in microwave applications.

ACKNOWLEDGEMENTS

We are grateful to NED University of Engineering and Technology, Karachi, Pakistan and ORIC of Balochistan University of Information Technology, Engineering and Management Sciences (BUITEMS), Quetta Pakistan for providing funds and lab facilities.

REFERENCES

[1] D. S. Mathew and R.-S. Juang, "An overview of the structure and magnetism of spinel ferrite nanoparticles and their synthesis in microemulsions," *Chemical engineering journal,* vol. 129, no. 1-3, (2007) pp. 51-65.

[2] A. Saini, P. Kumar, B. Ravelo, S. Lallechere, A. Thakur, and P. Thakur, "Magneto-dielectric properties of doped ferrite based nanosized ceramics over very high frequency range," *Engineering Science and Technology, an International Journal,* vol. 19, no. 2, (2016) pp. 911-916.

[3] R. C. Buchanan, *Ceramic materials for electronics*. CRC press, 2018.
[4] J. Jeevanandam, A. Barhoum, Y. S. Chan, A. Dufresne, and M. K. Danquah, "Review on nanoparticles and nanostructured materials: history, sources, toxicity and regulations," *Beilstein journal of nanotechnology,* vol. 9, no. 1, (2018) pp. 1050-1074.
[5] R. Ji, C. Cao, Z. Chen, H. Zhai, and J. Bai, "Solvothermal synthesis of Co x Fe 3− x O 4 spheres and their microwave absorption properties," *Journal of Materials Chemistry C,* vol. 2, no. 29, (2014) pp. 5944-5953.
[6] R. Valenzuela, "Novel applications of ferrites," *Physics Research International,* vol. 2012, 2012.
[7] R. Dosoudil, J. Franek, J. Slama, M. Usakova, and A. Gruskova, "Electromagnetic wave absorption performances of metal alloy/spinel ferrite/polymer composites," *IEEE transactions on magnetics,* vol. 48, no. 4, (2012) pp. 1524-1527.
[8] T. Tatarchuk, M. Bououdina, J. J. Vijaya, and L. J. Kennedy, "Spinel ferrite nanoparticles: synthesis, crystal structure, properties, and perspective applications," in *International Conference on Nanotechnology and Nanomaterials*, Springer, (2016) pp. 305-325.
[9] L. Leonel, A. Righi, W. Mussel, J. Silva, and N. Mohallem, "Structural characterization of barium titanate–cobalt ferrite composite powders," *Ceramics International,* vol. 37, no. 4, (2011) pp. 1259-1264.
[10] M. Cernea *et al.*, "Lead-Free BNT–BT0. 08/CoFe2O4 Core–Shell Nanostructures with Potential Multifunctional Applications," *Nanomaterials,* vol. 10, no. 4, (2020) p. 672.
[11] N. Singh, A. Agarwal, and S. Sanghi, "Dielectric relaxation, conductivity behavior and magnetic properties of Mg substituted Zn–Li ferrites," *Current Applied Physics,* vol. 11, no. 3, (2011) pp. 783-789.
[12] H. Wang, Y. Song, X. Ye, H. Wang, W. Liu, and L. Yan, "Asymmetric supercapacitors assembled by dual spinel ferrites@ graphene nanocomposites as electrodes," *ACS Applied Energy Materials,* vol. 1, no. 7, (2018) pp. 3206-3215.
[13] M. E. Hajlaoui, R. Dhahri, N. Hnainia, A. Benchaabane, E. Dhahri, and K. Khirouni, "Conductivity and giant permittivity study of Zn 0.5 Ni 0.5 Fe 2 O 4 spinel ferrite as a function of frequency and temperature," *RSC Advances,* vol. 9, no. 56, (2019) pp. 32395-32402.
[14] A. Arya and A. Sharma, "Structural, electrical properties and dielectric relaxations in Na+-ion-conducting solid polymer electrolyte," *Journal of Physics: Condensed Matter,* vol. 30, no. 16, (2018) p. 165402.[15] N. Sivakumar, A. Narayanasamy, B. Jeyadevan, R. J. Joseyphus, and C. Venkateswaran, "Dielectric relaxation behaviour of nanostructured Mn–Zn ferrite," *Journal of Physics D: Applied Physics,* vol. 41, no. 24, (2008) p. 245001.
[16] C. Henderson, J. Charnock, and D. Plant, "Cation occupancies in Mg, Co, Ni, Zn, Al ferrite spinels: a multi-element EXAFS study," *Journal of Physics: Condensed Matter,* vol. 19, no. 7, (2007) p. 076214.
[17] R. S. Yadav *et al.*, "Impact of grain size and structural changes on magnetic, dielectric, electrical, impedance and modulus spectroscopic characteristics of CoFe2O4 nanoparticles synthesized by honey mediated sol-gel combustion method," *Advances in Natural Sciences: Nanoscience and Nanotechnology,* vol. 8, no. 4, (2017) p. 045002.
[18] F. Li, J. Liu, D. G. Evans, and X. Duan, "Stoichiometric synthesis of pure MFe2O4 (M= Mg, Co, and Ni) spinel ferrites from tailored layered double hydroxide (hydrotalcite-like) precursors," *Chemistry of materials,* vol. 16, no. 8, (2004) pp. 1597-1602.
[19] S. Geller and M. Gilleo, "The crystal structure and ferrimagnetism of yttrium-iron garnet, Y3Fe2 (FeO4) 3," *Journal of Physics and Chemistry of solids,* vol. 3, no. 1-2, (1957) pp. 30-36.
[20] S. Raghuvanshi, F. Mazaleyrat, and S. Kane, "Mg1-xZnxFe2O4 nanoparticles: Interplay between cation distribution and magnetic properties," *AIP Advances,* vol. 8, no. 4, (2018) p. 047804.
[21] S. E. Shirsath, D. Wang, S. Jadhav, M. Mane, and S. Li, "Ferrites obtained by sol-gel method," in *Handbook of Sol-Gel Science and Technology*: Springer Cham, 2018, pp. 695-735.

[22] B. Toksha, S. E. Shirsath, S. Patange, and K. Jadhav, "Structural investigations and magnetic properties of cobalt ferrite nanoparticles prepared by sol–gel auto combustion method," *Solid State Communications,* vol. 147, no. 11-12, (2008) pp. 479-483.

[23] C. Murugesan, M. Perumal, and G. Chandrasekaran, "Structural, dielectric and magnetic properties of cobalt ferrite prepared using auto combustion and ceramic route," *Physica B: Condensed Matter,* vol. 448, (2014) pp. 53-56.

[24] S. Mourdikoudis, R. M. Pallares, and N. T. Thanh, "Characterization techniques for nanoparticles: comparison and complementarity upon studying nanoparticle properties," *Nanoscale,* vol. 10, no. 27, (2018) pp. 12871-12934.

[25] M. Bououdina and C. Manoharan, "Dependence of structure/morphology on electrical/magnetic properties of hydrothermally synthesised cobalt ferrite nanoparticles," *Journal of Magnetism and Magnetic Materials,* vol. 493,(2020) p. 165703.

[26] N. B. Velhal, N. D. Patil, A. R. Shelke, N. G. Deshpande, and V. R. Puri, "Structural, dielectric and magnetic properties of nickel substituted cobalt ferrite nanoparticles: Effect of nickel concentration," *AIP Advances,* vol. 5, no. 9,(2015) p. 097166.

[27] T. George, A. Sunny, and T. Varghese, "Magnetic properties of cobalt ferrite nanoparticles synthesized by sol-gel method," in *IOP Conference Series: Materials Science and Engineering*, IOP Publishing, vol. 73, no. 1, (2015) p. 012050.

[28] G. Brahmachari, S. Laskar, and P. Barik, "Magnetically separable MnFe 2 O 4 nano-material: an efficient and reusable heterogeneous catalyst for the synthesis of 2-substituted benzimidazoles and the extended synthesis of quinoxalines at room temperature under aerobic conditions," *RSC advances,* vol. 3, no. 34, (2013) pp. 14245-14253.

[29] B. Wang, G. Wang, Z. Lv, and H. Wang, "In situ synthesis of hierarchical CoFe 2 O 4 nanoclusters/graphene aerogels and their high performance for lithium-ion batteries," *Physical Chemistry Chemical Physics,* vol. 17, no. 40, (2015) pp. 27109-27117.

[30] A. Patterson, "The Scherrer formula for X-ray particle size determination," *Physical review,* vol. 56, no. 10, (1939) p. 978.

[31] A. M. Kumar, P. A. Rao, M. C. Varma, G. Choudary, and K. Rao, "Cation distribution in Co 0.7 Me 0.3 Fe 2 O 4 (Me= Zn, Ni and Mn)," *Journal of Modern Physics,* vol. 2011, 2011.

[32] S. K. Gore *et al.*, "Influence of Bi 3+-doping on the magnetic and Mössbauer properties of spinel cobalt ferrite," *Dalton Transactions,* vol. 44, no. 14, (2015) pp. 6384-6390.

[33] M. Junaid *et al.*, "Structural, spectral, dielectric and magnetic properties of Tb–Dy doped Li-Ni nano-ferrites synthesized via micro-emulsion route," *Journal of Magnetism and Magnetic Materials,* vol. 419, (2016) pp. 338-344.

[34] C. Koops, "On the dispersion of resistivity and dielectric constant of some semiconductors at audiofrequencies," *Physical review,* vol. 83, no. 1, (1951) p. 121.

[35] K. Wagner, "Dissipation of energy under AC," *Ann. Phys,* vol. 40, pp. 817-855, 1913.

[36] M. Costa, G. Pires Jr, A. Terezo, M. Graca, and A. Sombra, "Impedance and modulus studies of magnetic ceramic oxide Ba2Co2Fe12O22 (Co2Y) doped with Bi2O3," *Journal of Applied Physics,* vol. 110, no. 3, (2011) p. 034107.

[37] A. Sinha and A. Dutta, "Microstructure evolution, dielectric relaxation and scaling behavior of Dy-for-Fe substituted Ni-nanoferrites," *RSC advances,* vol. 5, no. 121, (2015) pp. 100330-100338.

[38] J. Baraliya and H. Joshi, "Spectroscopy investigation of nanometric cobalt ferrite synthesized by different techniques," *Vibrational Spectroscopy,* vol. 74, (2014) pp. 75-80.

[39] P. Chandramohan, M. Srinivasan, S. Velmurugan, and S. Narasimhan, "Cation distribution and particle size effect on Raman spectrum of CoFe2O4," *Journal of Solid State Chemistry,* vol. 184, no. 1, (2011) pp. 89-96.

[40] T. Yu, Z. Shen, Y. Shi, and J. Ding, "Cation migration and magnetic ordering in spinel CoFe2O4 powder: micro-Raman scattering study," *Journal of Physics: Condensed Matter,* vol. 14, no. 37, (2002) p. L613.